



ELSEVIER

Microelectronic Engineering 63 (2002) 147–153

MICROELECTRONIC  
ENGINEERING

www.elsevier.com/locate/mee

## Spintronics with Si quantum dots

Leonid P. Rokhinson\*, Lingue J. Guo, Steven Y. Chou, Daniel C. Tsui

*Department of Electrical Engineering, Princeton University, Princeton, NJ 08544, USA*

---

### Abstract

Electron transport through small Si quantum dot is investigated. The  $B$ -dependence of energy levels is dominated by the Zeeman shift, allowing us to measure the spin difference between two successive ground states directly. Combined with the ability to change the number of electrons  $N$  in the dot between 0 and 30, we are able to map the spin of the the dot as a function of  $N$  and  $B$ . Various spin-related phenomena, such as singlet–triplet transitions and spin blockade, are observed. © 2002 Elsevier Science B.V. All rights reserved.

*Keywords:* Quantum dots; Si nanostructures; Spin blockade; Coulomb blockade

---

### 1. Introduction

In most of the practical devices, spin, which doubles the degeneracy of energy levels at zero magnetic field, is an elusive property. There are just a few phenomena, such as the Kondo effect, where a single spin fundamentally changes the macroscopic properties of the system. Recent proposals on spin-based qubits (for a review of proposals for quantum computation with quantum dots, see Ref. [1]) have renewed our interest in spin phenomena with very demanding challenges for single spin detection, manipulation, and for the precise control of spin interactions. Over the last year, we have shown that most of these goals can be achieved with small Si quantum dots [2–4]. Moreover, we showed that coherence can be preserved during the charge transfer through a Si double-dot dimer [5].

### 2. Samples

Small Si quantum dot devices are fabricated from a silicon-on-insulator wafer. A narrow bridge with a lithographically defined dot is formed from the top Si layer; the bridge is connected to wide

---

\*Corresponding author. Present address: Department of Electrical Engineering and Computer Science, University of Michigan, Ann Arbor, MI 48109, USA.

*E-mail address:* [leonid@ee.princeton.edu](mailto:leonid@ee.princeton.edu) (L.P. Rokhinson).

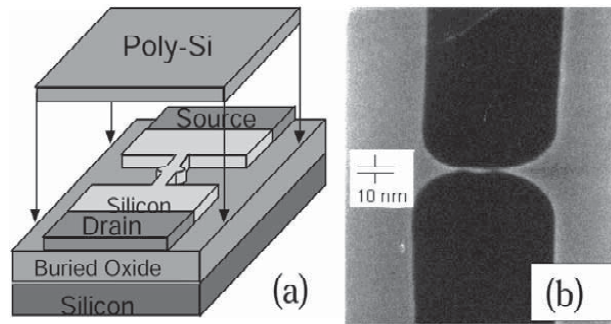


Fig. 1. (a) Three-dimensional schematic of the device structure and (b) SEM micrograph.

source and drain regions via two constrictions (see Fig. 1). Subsequently, a 50-nm thick layer of  $\text{SiO}_2$  is thermally grown around the dot, followed by a poly-Si gate (for a detailed description of sample preparation, see Ref. [6]). In most cases, more than one dot is formed in such Si nanostructures and, most probably, the origin of these additional dots are traps in the gate oxide [7–9]. We were able to make a few devices that exhibit single dot transport down to the lowest temperature  $T = 50$  mK.

### 3. Electron counting

Counting of electrons in quantum dots is not a straightforward task. The onset of Coulomb blockade (CB) oscillations does not necessarily indicate the entrance of the first electron, especially if transparency of the tunneling barriers depends on the gate voltage  $V_g$ . In principle, the number of electrons,  $N$ , in dots with well defined geometry can be determined by comparing the experimental and theoretically expected energy spectra. In practice,  $N$  was determined in circular dots with parabolic confinement by matching the measured  $B$  dependence of energy levels with the expected evolution for the Darwin–Fock states [10,11]. This method cannot be used for dots with unknown geometry; also, it fails for dots with strong confinement, where the  $B$  dependence is dominated by Zeeman, rather than orbital, effects.

We used the information obtained from high bias spectroscopy, field-dependence of energy levels and conductance at elevated temperatures to determine the number of electrons in our dot. At room temperature, the device behaves as a regular MOSFET with a cutoff at  $-0.2$  V (Fig. 2c). Thus, we are expecting the dot to be empty at  $V_g < -0.2$  V. Results of the high-bias spectroscopy, performed at 1.2 K, are shown in Fig. 2b, and the peak positions are outlined in Fig. 2a for clarity. The spectrum is much more complicated than the ones reported for GaAs quantum dots (for a recent review, see Ref. [12]) and reflects both non-regular geometry of the sample and complexity of the conduction band of Si. As indicated by the dashed lines in Fig. 2a, there should be two more peaks at 0.13 and  $-0.03$  V which are not resolved at zero bias. It is unlikely that there are any more missing peaks between  $-0.03$  and  $-0.2$  V, since the average peak spacing is  $\sim 0.2$  V and the onset of the conductance is expected to shift to higher  $V_g$  at low temperatures. However, there is one more indication that, indeed, the first electron is added into the dot at  $-0.03$  V.

Electrostatically, peak shifts in the  $V_b - V_g$  plane are determined by the ratios of source, drain and gate capacitances,  $C_g/C_s$  and  $-C_g/(C_d + C_g)$ . These ratios increase gradually as  $V_g$  increases. This

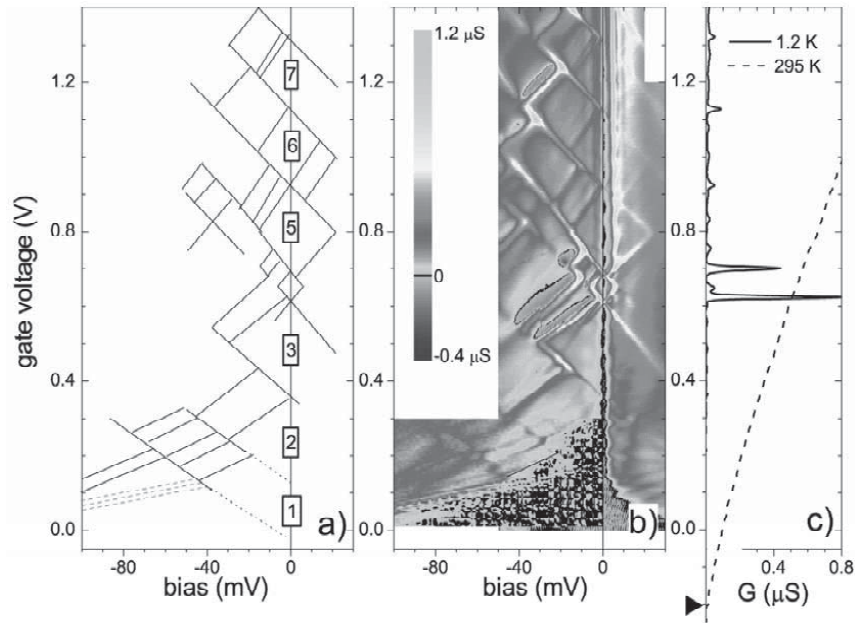


Fig. 2. Differential conductance measured at 1.2 K. In (a) peak positions from (b) are outlined, the numbers indicate the total number of electrons in the dot at  $V_b = 0$ . In (c) conductance at  $V_b = 0$  is plotted for  $T = 1.2$  and 295 K; triangle indicates the onset of the conductance at room temperature.

increase can be attributed to a decrease of the tunneling barriers and the corresponding increase of  $C_s$  and  $C_d$ . However, the slope of the dashed lines in Fig. 2a, which separate regions with zero and non-zero conductance, is  $\sim 5$  times different from the slope of the solid lines nearby. We attribute this slope difference to the ill-defined capacitances in the empty dot in the region below the dashed lines.

As a final check of our electron counting, we compare peak broadening of neighboring peaks. Peaks 4 and 5 (the two large peaks) are fitted to a Lorentzian function convoluted with the Fermi–Dirac thermal broadening at 50 mK. Peak 4 has negligible coupling to the leads  $\Gamma_4 < 0.5 \mu\text{eV}$ , while, for peak 5,  $\Gamma_5 = 2.5 \mu\text{eV}$ . Different coupling of energy levels reflects difference in spatial distribution of the wavefunctions, and, thus, confirms that these two peaks belong to different energy levels, as expected for peaks 4 and 5.

#### 4. Expected field dependence of the energy levels

At zero bias the conductance is non-zero only when the electrochemical potential of the dot equals the electrochemical potential of the leads. Within the constant interaction model, the peak position  $V_g^p$  is determined by the condition [13]:

$$\frac{e^2}{C} - \frac{eC_g}{C} V_g^p(B) + E_N(B) + [S_z(N) - S_z(N-1)] g^* \mu_B B = E_F(B)$$

where the first term is the charging energy, the third term is the kinetic energy of the state with  $N$  electrons, the fourth term is the Zeeman energy [usually  $|S_z(N) - S_z(N-1)| = 1/2$ ], and  $E_F$  is the Fermi

energy in the leads.  $E_F$  is field independent as long as the contacts are not spin-polarized. The contacts become polarized at a critical field  $B_c$  when  $E_F(0) = \frac{1}{2}g^*\mu_B B_c$ , and, for  $B > B_c$ ,  $E_F(B) = E_F(0) - \frac{1}{2}g^*\mu_B B$ . The  $B$ -dependence of  $E_N(B)$  is suppressed in our samples due to the strong electron confinement provided by the Si/SiO<sub>2</sub> interface [3]). Thus, at low fields  $B < B_c$ , we expect  $V_g^p(B)$  to have a linear  $B$  dependence. At  $B > B_c$ , the Zeeman terms on the left and the right hand sides of the equation cancel and  $V_g^p(B)$  reflects the weak field dependence of  $E_N(B)$ .

## 5. Spin transitions in a few-electron regime

For  $V_g < 0.4$  V (the first three peaks), the electron density in the contacts is low and the contacts are spin-polarized in a moderate magnetic field,  $B_c < 13$  T. At  $B > B_c$ , the peaks positions become almost field independent [3], as expected for the strong confinement.

For  $V_g > 0.4$  V ( $N \geq 4$ ), both spin subbands in the contacts are occupied within the experimental range of  $0 < B < 13$  T, the  $E_F$  is field independent and the peak shift reflects only the field dependence of the energy levels in the dot (also, mobility of the two-dimensional gas is low,  $\approx 300$  cm<sup>2</sup> V<sup>-1</sup> s<sup>-1</sup> at 4.2 K, and there is no measurable modulation of  $E_F$  due to Shubnikov–de Haas oscillations for  $B$  up to 13 T).

The peak position as a function  $B$  is plotted in Fig. 3 for peaks 4–7.  $V_g^p$  was found to be insensitive to the direction of  $B$ : aligning  $B$  with the current direction ( $B_{||}$ , in-plane) or perpendicular to the plane of the sample ( $B_{\perp}$ ) does not change  $V_g^p$  significantly. Our lithographically defined dot is elongated along the bridge axis and orbital effects are expected to depend on the direction of  $B$ . Thus, the  $B$ -dependence of  $V_g^p$  is dominated by spin effects.

For a quantitative analysis, the peak positions are extracted from  $G$  vs.  $V_g$  scans, and the peak shift,  $\Delta U^p(B) = [V_g^p(B) - V_g^p(0)]/\alpha$ , is plotted as a function of  $B$  in Fig. 3b. The curves are offset for clarity. For comparison, lines with slopes  $\pm 1/2g^*\mu_B$  for  $g^* = 2$  are also shown (solid lines). First, let us focus on the low field ( $B < 2$  T) region. Peaks 4 and 5 shift linearly with  $B$  and the corresponding slopes are + and  $-1/2g^*\mu_B$ . In the same low field region the preceding peaks 2 and 3 also shift with + and  $-1/2g^*\mu_B$  slopes. Thus, at low fields the ground states with up to five electrons in the dot have the lowest spin configuration and the dot is filled in a spin-down–spin-up sequence. Such a filling sequence requires that the valley degeneracy is lifted.

The low-field spin configuration is not preserved at higher magnetic fields. For peak 4,  $dV_g^p/dB$  changes sign from positive to negative at  $B = 2.5$  T, back to positive at  $B = 9$  T, and, again, to negative at  $B \approx 12$  T. The spin of the tunneling electron changes from being  $+1/2 \rightarrow -1/2 \rightarrow +1/2 \rightarrow -1/2$ . The corresponding spin transitions of the ground state can be understood from a simple model for non-interacting electrons. Let us consider four single particle levels  $E_i$ , as shown in Fig. 3c. Each level is spin-degenerate at zero field and splits into two levels  $E_i \pm 1/2g^*\mu_B B$  for  $B > 0$ . The 4th ground state  $E_4(B)$  should follow the thick solid line in Fig. 3c. Qualitatively,  $E_4(B)$  captures the main features of  $V_g^p$  vs.  $B$  for the 4th peak and the kinks can be attributed to the corresponding level crossings. The first kink at  $B = 2.6$  T marks the singlet–triplet transition and the kink at 11 T corresponds to the transition from a triplet to a spin-polarized state. The singlet–triplet transition is not an exchange-driven transition, as in previously reported studies [14–16], but is a result of the

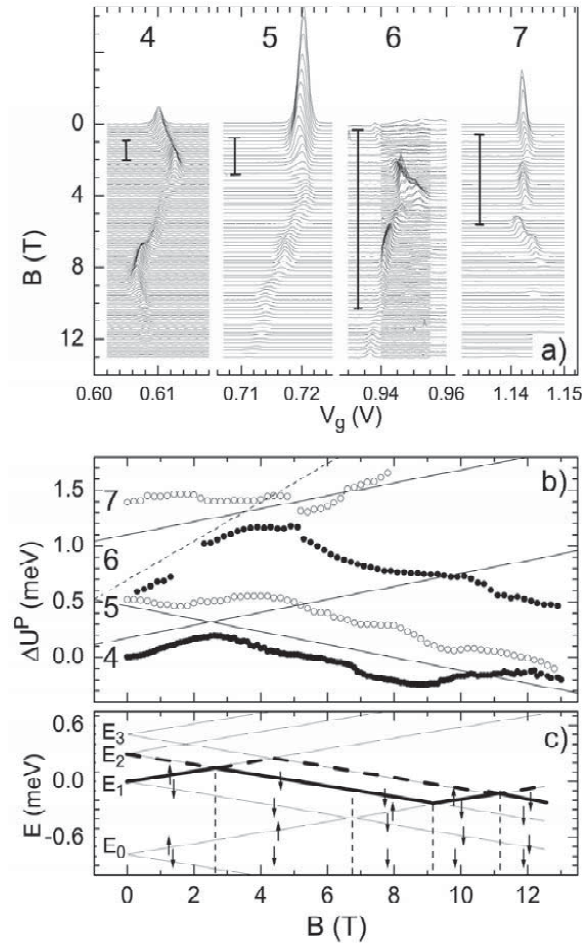


Fig. 3. (a) Conductance for four consecutive peaks was measured at 200 mK with  $V_{ac} = 50 \mu\text{V}$ . Individual traces are offset linearly with  $B$  and the vertical bars are  $1 \mu\text{S}$  scales. In (b), peak shifts  $\Delta U^P(B) = [V_g^P(B) - V_g^P(0)]/\alpha$  are plotted for the same four peaks. The zero-field positions are arbitrarily offset. Points are omitted if the peak conductance is  $< 0.01 \mu\text{S}$ . Solid and dashed lines have slopes  $1/2$  and  $3/2g^* \mu_B$ , respectively. (c) Schematic evolution of single-particle energy levels, assuming only the Zeeman level splitting.

crossing of levels with different spins. As a result, the energy difference between the singlet and the triplet states can be continuously and controllably tuned by adjusting the magnetic field.

There are two kinks within the triplet state which do not change the total spin of the four-electron state. Below  $B = 9 \text{ T}$  the 4th electron tunnels into  $E_2^\downarrow$  level, while above  $9 \text{ T}$  into  $E_0^\uparrow$  level, reversing its spin. At the same time the three-electron state undergoes a transition from  $S(3) = 1/2$  to  $3/2$ , conserving the total spin of a four-electron state  $S(4) = 1$ . The kink at  $B = 7 \text{ T}$ , which coincides with the crossing of  $E_0^\uparrow$  and  $E_1^\downarrow$ , is a small offset, which does not change the sign of  $dV_g^P/dB$ . In the absence of interactions there should be no corresponding kink.

There are small deviations from the predictions of the single-particle level crossing model. For example, there is a  $\sim 0.5 \text{ T}$  shift in the upward kink in peak 4 and downward kink in peak 5 at around  $2.3 \text{ T}$ . This deviation can be accounted for by considering exchange interactions [17].

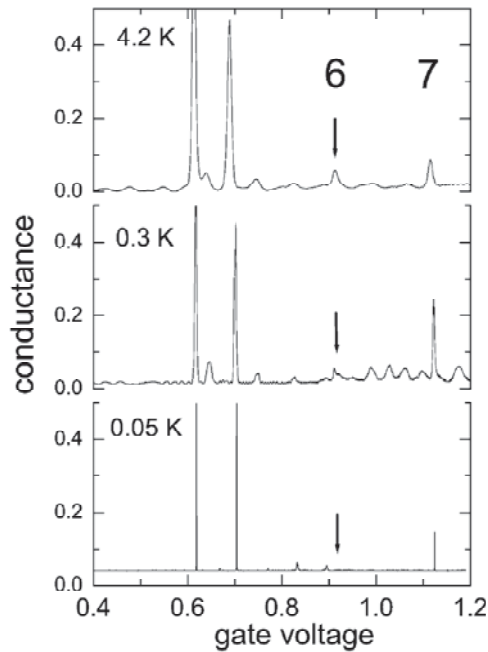


Fig. 4. Conductance is plotted as a function of the gate voltage for different temperatures. Arrows indicate position of peak 6.

## 6. Spin blockade

The simple picture of alternating filling does not hold for  $N > 5$  even at low fields. At  $B < 2$  T, peak 6 shifts with a slope close to  $3/2g^*\mu_B$ . The shift of the next, the 7th, peak has a positive slope, while the lowest spin configuration for a dot with seven electrons should have a negative Zeeman shift. We conclude that the ground state with six electrons in the dot is spontaneously polarized and the total spin  $S_z(6) > 1/2$ . Moreover, the spin change  $|S_z(6) - S_z(5)| = 3/2$ . Transitions between ground states that involve a spin change  $\Delta S_z > 1/2$  require spin-scattering mechanism in order to conserve the total angular momentum and the corresponding peaks are expected to be suppressed [18] (so-called spin blockade). Indeed, peak 6 is suppressed at low temperatures by more than two orders of magnitude (see Fig. 4).

## 7. Spin transitions for large $N$

At larger  $N \geq 19$ , the energy spectrum is completely dominated by interactions and changes entirely as electrons are added into the dot. For example, the basic prediction of the level crossing model is an appearance of a kinks and an anti-kink in the field evolution of two neighboring peaks at the value of  $B$  when the two energy levels cross. This prediction is grossly violated for large  $N$  and some kinks do not have a counterpart. At the same time, field evolution of some peaks indicates large spin change  $\Delta S_z = 3/2$  without an apparent suppression of the peak height! This lifting of the spin blockade is not yet understood.

## 8. Conclusions

We discussed spin-related phenomena in small Si quantum dots. Using the dot whose electron confinement is so strong that the  $B$ -dependence of its energy levels is dominated by the Zeeman energy, we are able to measure spin directly. We can identify and follow the evolution of the total spin of the dot as a function of the magnetic field and electron number. Due to interaction effects some transitions involve spin changes  $\Delta S > 1/2$ . The large change in spin results in spin blockade and the corresponding suppression of peaks at low  $T$  for small number of electrons in the dot.

## Acknowledgements

The authors acknowledge financial support from ARO, ONR and DARPA and by the MARCO Focused Research Center on Materials, Structures and Devices which is funded at the MIT, in part by MARCO under contract 2001-MT-887 and DARPA under grant MDA972-01-1-0035.

## References

- [1] G. Burkard, H.-A. Engel, D. Loss, *Fortschritte der Physik* 48 (2000) 965.
- [2] L.P. Rokhinson, L.J. Guo, S.Y. Chou, D.C. Tsui, *Phys. Rev. B* 63 (2001) 035321, cond-mat/0005262.
- [3] L.P. Rokhinson, L.J. Guo, S.Y. Chou, D.C. Tsui, in: N. Miura, T. Ando (Eds.), *Proceeding of the 25th International Conference on the Physics of Semiconductors*, Osaka, Japan, 2000, Springer, New York, 2001, p. 1021, cond-mat/0102107.
- [4] L.P. Rokhinson, L.J. Guo, S.Y. Chou, D.C. Tsui, *Phys. Rev. Lett* 87 (2001) 166802, cond-mat/0108210.
- [5] L.P. Rokhinson et al., *Phys. Rev. Lett.* 88 (2002) 186801.
- [6] E. Leobandung, L.J. Guo, Y. Wang, S.Y. Chou, *J. Vac. Sci. Technol.* 13 (1995) 2865.
- [7] L.P. Rokhinson, L.J. Guo, S.Y. Chou, D.C. Tsui, *Appl. Phys. Lett.* 76 (2000) 1591.
- [8] L.P. Rokhinson, L.J. Guo, S.Y. Chou, D.C. Tsui, *Superlattices Microstruct.* 28 (2000) 413.
- [9] R. Ludeke, E. Cartier, *Appl. Phys. Lett.* 78 (2001) 3998.
- [10] B. Su, V.J. Goldman, J.E. Cunningham, *Phys. Rev. B* 46 (1992) 7644.
- [11] R.C. Ashoori et al., *Phys. Rev. Lett.* 71 (1993) 613.
- [12] L.P. Kouwenhoven, L.L. Sohn, G. Schön (Eds.), *Mesoscopic Electron Transport*, NATO ASI Series E, Vol. 345, Kluwer, London, 1997.
- [13] C.W.J. Beenakker, *Phys. Rev. B* 44 (1991) 1646.
- [14] R.C. Ashoori, J.A. Lebens, N.P. Bigelow, R.H. Silsbee, *Phys. Rev. B* 48 (1993) 4616.
- [15] T. Schmidt et al., *Phys. Rev. B* 51 (1995) 5570.
- [16] W.G. Van der Wiel et al., *Physica B* 256–258 (1998) 173.
- [17] I.L. Kurland, R. Berkovits, B.L. Altshuler, *Phys. Rev. Lett.* 86 (2001) 3380.
- [18] D. Weinmann, W. Häusler, B. Kramer, *Phys. Rev. Lett.* 74 (1995) 984.